ISSN 2079-1704. Хімія, фізика та технологія поверхні. 2025. Т. 16. № 3. С. 425-437

UDC 544.47+546.215+546.655 doi: 10.15407/hftp16.03.425

A.M. Hrynko [1, 2], A.V. Brichka [2], O.M. Bakalinska [1, 2], H.O. Kaleniuk [2], M.T. Kartel [2]

HYDROGEN PEROXIDE DECOMPOSITION BY NANOCOMPOSITES HALLOYSITE NANOTUBES/CERIUM OXIDE

[1] National University of "Kyiv-Mohyla Academy"
2 Skovorody Str., Kyiv, 04070, Ukraine, E-mail: alinagrinko2@gmail.com
[2] Chuiko Institute of Surface Chemistry of National Academy of Sciences of Ukraine
17 Oleh Mudrak Str., Kyiv, 03164, Ukraine, E-mail: bakalin2008@ukr.net

A number of nanomaterials based on halloysite nanotubes (HNT) decorated with CeO_2 were synthesized by the precipitation method of aqueous cerium nitrate at room temperature without stabilizers in the presence of HNT. The amount of nanoceria deposited in nanomaterials ranges from 0.99 to 19.15 % wt. Electron microscopy has shown that the size of CeO_2 particles varies in the range of 2.6–17.5 nm. The cubic structure of cerium dioxide has been shown by X-ray diffraction analysis of the samples. The characteristics of the porous structure were determined based on low-temperature nitrogen adsorption/desorption isotherms. The specific surface area ranged from 31 to 54 m^2/g. IR spectroscopy determined the type of interaction between the modifier and the matrix. The $I_{UVS\ Ce^{4+}}/I_{UVS\ Ce^{3+}}$ ratio in nanocomposites was estimated from UV-spectra of diffuse reflectance; it varied in the range of 0.25 to 2.55. The catalytic activity of the synthesized materials and halloysite nanotubes was determined by calculating the affinity constant from kinetic data of the model reaction of hydrogen peroxide decomposition in the pH range of 8.0 to 11.0 and compared to the catalase enzyme and commercial nanosized CeO_2. The catalytic activity of pristine HNT decreased with increasing pH. We can assume that the activity of the synthesized nanocomposites at pH range 9.0–11.0 is determined by the presence and properties of a decorator – nanoceria. The pH dependence of the activity of the nanocomposites was shown to be extreme with the maximum in the pH range of 9.5–10.5. An extreme dependence of the activity on the content of the decorator with a maximum for the sample of 3.19 % wt. CeO_2 was found. Recalculation of the catalytic capability of nanocomposites to 100 % of the content of the decorator in them makes it possible to analyze the factors that determine the activity of nanoceria. Under these conditions, the best catalytic activity demonstrates by sample HNT-1CeO_2, which contains 0.99 % wt. of the modifier and has a ratio of Ce^{4+}/Ce^{3+} 0.25. It was found that the activity of nanoceria in nanocomposites decreases with: increasing Ce^{4+}/Ce^{3+} ratio, i.e. with decreasing the number of oxygen vacancies; with increasing cerium oxide content - due to aggregation of nanocrystallites; and with increasing particle diameter due to the reduction of the surface. The activation energy (E_a) of the reaction of hydrogen peroxide decomposition by the nanocomposites and pristine HNT in the temperature range of 20–40 °C at pH 10 was determined by kinetic data. The E_a for pristine HNT is 170 kJ/mol. It has been shown that the increasing content of nanoceria in nanocomposites leads to a decrease in the activation energy of the reaction of hydrogen peroxide decomposition from 154 kJ/mol for the material with the lowest modifier content to 112 kJ/mol for the nanocomposite with the highest amount of a modifier.

***Keywords**: cerium oxide nanoparticles, halloysite nanotubes, nanocomposites, catalytic activity, hydrogen peroxide decomposition, activation energy*

INTRODUCTION

Tubular nanomaterials are widely used for the creation of organic and inorganic nanocomposites because they have high hydrodynamic and aerodynamic characteristics. Halloysite nanotubes (HNTs) have a structure similar to carbon nanotubes, but they are eco-friendly, have higher biocompatibility and lower cost [1]. Halloysite is a natural aluminosilicate mineral clay that has a hollow tubular structure. The chemical formula for HNTs is $Al_2Si_2O_5(OH)_4 \cdot nH_2O$, where n = 0–2. The mineral contains impurities of associated particles of other minerals, iron and titanium oxides, cations of potassium, sodium, calcium, magnesium, and natural organic compounds. The length of HNTs is approximately 500 to 1500 nm, the outer diameter is approximately 40 to 70 nm, the inner diameter is 10 to 20 nm [2]. The layered structure of HNTs consists of tetrahedral (Si-O) and octahedral (Al-O) linked sheets. Siloxane groups (Si–O–Si) are located on the external surface. A small number of silanol (Si-OH) and aluminol (Al-OH) groups are formed on the edges and surface

defects of HNTs. The surface internal lumen is composed of aluminol groups (Al–OH) that may be localized in the cavities of nanotubes. The chemical differences in surface structures lead to the formation of positive zeta potential for the inner surface and negative zeta potential for the outer surface depending on pH [3]. Halloysite materials have the same chemical composition as kaolin, dickit, cover, but have a different structure. A feature of halloysite compared to other similar minerals is the amount of water that is located between the layers of a crystalline solid: water molecules bind to the moist layers of the walls, acting as an adhesive between them [4]. These structural features of HNTs make it possible to modify the interlayer space and the inner and outer surfaces of the nanotubes to obtain nanocomposite catalysts with predictable properties [5]. The outer siloxane surface is negatively charged, porous, and unsuitable for modification with organic molecules [6]. However, it can be modified with nanoparticles of metals and their oxides, making it possible to create effective catalysts for use in various systems [7]. The aluminol groups on the inner surfaces of the HNTs actively react with organic molecules, for example, with organosilicon. Despite the strong hydrogen bonds between the aluminosilicate layers, some organic and inorganic molecules are capable of intercalating directly into the interlayer space [6]. These nanocomposites can be used in the biomedical industry because they are biocompatible and provide prolonged release of modifier nanoparticles from the interlayer space for several days and months after application [8].

Cerium is a rare earth metal, with atomic number 58, the second element of the group of lanthanides. Cerium oxide nanoparticles are being actively studied as promising agents for catalysis, photocatalysis, solar cells, SOFCs, optical devices, and UV absorbers due to their unique redox properties. The capability of CeO_2 nanoparticles to scavenge effectively reactive oxygen species is used in the biomedical field to treat effects caused by oxidative stress, such as Parkinson's, Alzheimer's, Huntington's, multiple sclerosis, ischemia, traumatic brain injury, aging, and as therapeutic and antibacterial agents. Nanoceria can exhibit catalytic activity similar to the enzymes catalase, superoxide dismutase, peroxidase, oxidase, and phosphatase depending on the pH of the medium. At the nanoscale, both Ce^{3+} and Ce^{4+} ions coexist on the particle surface and they can switch between three- and four oxidation states. It leads to the formation of surface vacancy sites, which are responsible for the high catalytic activity of cerium oxide nanoparticles. Increasing the surface-to-volume ratio is accompanied by an increase in the concentration of Ce^{3+} ions and to compensate for a charge deficiency, oxygen defects are created. The catalytic activity of CeO_2 nanoparticles is affected by various factors, including size, morphology, pH and surface defects concentration, which are defined as the ratio of Ce^{4+}/Ce^{3+} ions. Modification of substrates with nanoceria allows improving the characteristics of the obtained nanoparticles and reducing agglomeration between them, which has a positive effect on the catalytic activity [9–11].

Nanocomposites based on nanoceria and HNTs have shown a remarkable prospect for application as orally drug delivery system [12, 13], as catalysts [14], corrosion inhibition composite coatings [15], for membrane modification [16]. The authors [17] synthesized a number of HNT/CeO_2 nanocomposites with different modifier content for UV protection. We decided to use this method to synthesize a number HNT-based nanocomposites with different content of nanoceria, analyze their physicochemical properties, aiming to experimentally determine the catalytic enzyme-like activity of the synthesized materials in a model reaction of hydrogen peroxide decomposition at different pH medium, to find the effective activation energy of the reaction of hydrogen peroxide decomposition by synthesized nanocomposites, pristine halloysite nanotubes and nanoceria.

MATERIALS AND METHODS

Nanocomposites were synthesized by the chemical deposition of cerium oxide in an alkaline medium from aqueous solutions with the presence of halloysite nanotubes (NaturalNano, Inc.) according to the reaction:

$$4Ce(NO_3)_3+12NaOH+O_2 = 4CeO_2+12NaNO_3+6H_2O.$$

The nanocomposite suspension was filtered, washed, and dried at 383 K. The samples of HNTs/CeO_2 were synthesized with different cerium oxide nanoparticles content in nanocomposites 1, 3, 5, 12, and 20 % wt. and designated as HNT-1CeO_2, HNT-3CeO_2, HNT-5CeO_2,

HNT-12CeO_2 and HNT-20CeO_2, respectively. The samples were characterized according to the scanning (MIRA3 LMU, TESCAN) and transmission (Hitachi H-800) electron microscope images using electron diffraction in the selected area. The porous texture was determined from nitrogen adsorption isotherms measured at 77.4 K with a NOVA 2200 (Quantachrome). The specific surface area of the nanocomposites was calculated using the BET method. The amount of nitrogen adsorbed at relatively pressure of $p/p_0 = 0.95$ was employed to determine the total pore volume. Nitrogen desorption isotherm profiles were used by the DFT method to assess the volume and size of pores. A Thermo Nicolet Nexus FT-IR spectrometer was used to record the IR spectra of HNT and nanocomposites in the range of 4000–400 cm^{-1} in diffuse reflection mode with a measurement uncertainty of ±1.8 cm^{-1} at room temperature.

The enzyme mimetic activity of the pristine HNT and nanoceria-containing materials and the effective activation energy of the reaction were determined in a model reaction of the decomposition of hydrogen peroxide. A volumetric method was used to examine the kinetics of the decomposition of hydrogen peroxide. The initial concentration of hydrogen peroxide in solutions was determined by permanganometric titration. The experiment was conducted for 30 min with a constant stirring of the reaction mixture having a total volume of 25 mL. The volume of oxygen released was fixed with a precision of 0.02 mL. The numerical determination and comparison of the catalase activity of nanomaterials and the enzyme catalase were made using the concepts of the enzyme reactions with the Michaelis constant (K_m, mM). The maximum reaction rate was determined from the kinetic data of the decomposition of substrate solutions with a concentration of 1–10 % in the pH range of 8.0 to 11.0 (borate buffer) by the optimal catalyst weight. The Michaelis constant was determined from the plot of the maximum reaction rate versus concentration in the double reciprocal Lineweaver–Burk coordinates. The reliability of the approximation of the linearization of the experimental data in almost all cases exceeds 0.9. To facilitate the interpretation of the obtained experimental data, the affinity constant (K_{af}, mM^{-1} reverse to the Michaelis constant) was used. The activation energy of the reaction was determined based on the dependence of the reaction rate constant (k, s^{-1}) on the reciprocal temperature. To determine the activation energy of the reaction of the decomposition reaction of hydrogen peroxide, the experiments were carried out at the temperatures of 20, 25, 30, 35, 40 °C (pH 10.0).

RESULTS AND DISCUSSION

The porous structure of the prepared samples was studied by nitrogen physical adsorption/desorption measurements. The distribution of pores by size for the pristine halloysite nanotubes and the synthesized HNT/CeO_2 nanocomposites (Fig. 1 *a*) indicates that the porosity of the nanocomposites is determined by the structure of the pristine HNT. According to the classifcation of the International Union of Pure and Applied Chemistry, the adsorption curve (Fig. 1 *b*) belongs to the type IV a adsorption isotherm, with a distinct hysteresis loop, indicating capillary condensation in the mesopores. The profile of the hysteresis loop can be attributed to the H3 type. It is believed that the type of hysteresis H3 is associated with the slit-like shape of the pores.

The specific surface area and pore size of the synthesized material are important factors in determining the catalytic activity. The BET specific surface areas (S_{BET}), pore volumes (V_P) and DFT pore sizes are calculated from the isotherms (Table 1). The surface area, S_{BET}, of HNT is 31 m^2/g and for nanocomposites varies from 43 to 57 m^2/g. The total pore volume for pristine HNTs is 0.23 cm^3/g and for modified with nanoceria increases within the range of 0.33–0.45 cm^3/g.

The catalytic activity of the material is determined by the dispersion and particle distribution of the modifier in the nanocomposite. TEM images of synthesized materials in light and dark fields show small particles of nanoceria deposited on elongated particles of aluminosilicates (Fig. 2). TEM images of synthesized materials in light and dark fields provide. A dark field TEM image was used to determine the sizes of cerium oxide nanoparticles as more contrasting ones.

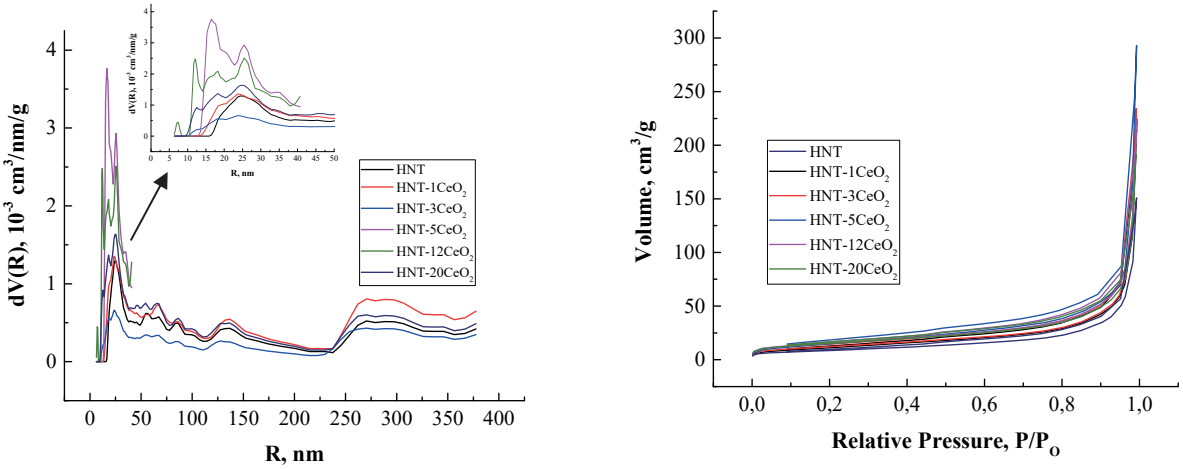

a *b*

Fig. 1. Pore distribution of HNT-CeO_2 nanocomposites by size (DFT) (*a*); Nitrogen adsorption-desorption isotherms by nanocomposites HNT-CeO_2 (*b*)

Table 1. Structural and sorption characteristics of nanocomposites HNT – CeO_2

Material	S_{BET}, m^2/g	V_P, cm^3/g	R_{pore}, nm (DFT)
HNT	31	0.23	24
HNT-1CeO_2	43	0.33	24
HNT-3CeO_2	45	0.36	24
HNT-5CeO_2	57	0.45	17
HNT-12CeO_2	55	0.35	25
HNT-20CeO_2	54	0.30	25

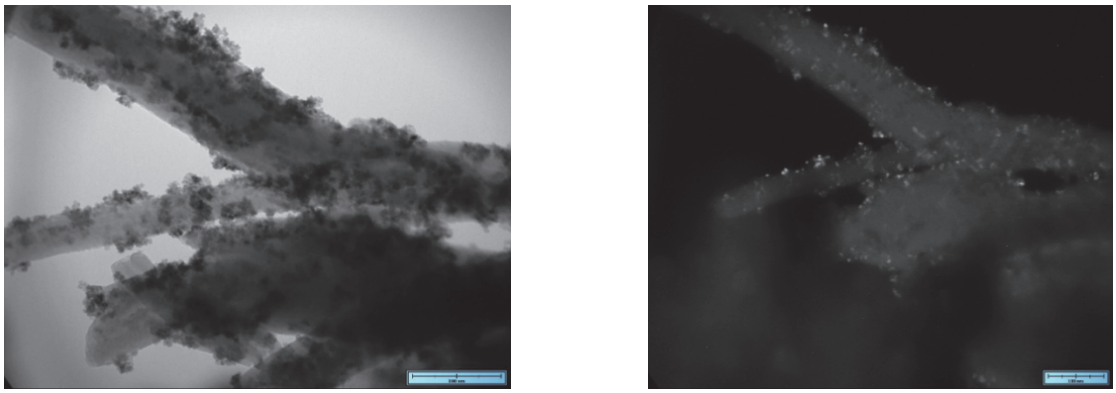

a *b*

Fig. 2. TEM images in light (*a*) and dark (*b*) field of HNT-20CeO_2 nanocomposites

The content of CeO_2 in the synthesized samples varies within the range of 0.99 to 19.15 %. The analysis of images of nanocomposites with different content of nanoceria has shown that an increase in the concentration of the modifier during the process of synthesis leads to the formation of larger decorator particles (Table 2). We conclude that the nanoscale carrier has a templating effect. The small size of cerium particles is also explained by the fact that a significant number of heterogeneous contacts between nanotubes contribute to the crystallization of small particles.

Electron diffraction studies of modifying particles in the samples revealed reflexes d(hkl) = 3.12(111), 2.7(200), 1.89(220), and

1.64 Å (311), which indicates the cubic structure of cerium dioxide (Fig. 3). The significant blurring of modifier signals can be explained by the influence of the nanosized crystallites and the low crystallinity of nanoceria.

Table 2. Particle sizes and content of nanoceria and H_2O in HNT/CeO_2 nanocomposites

Material	Particle size distribution, nm	CeO_2 content, %	$I_{UVS\ Ce^{4+}}/I_{UVS\ Ce^{3+}}$ in UV-spectra of nanocomposite	E_a, kJ/mol
HNT (d = 30–70 l = 250–4000)	–	0.00	–	170
HNT-1CeO_2	ND*	0.99±0.01	0.25	154
HNT-3CeO_2	4.95 (2.6–7.3)	3.19±0.02	1.17	145
HNT-5CeO_2	7.40 (3.9–10.9)	4.89±0.06	1.40	142
HNT-12CeO_2	ND*	12.17±0.21	2.02	132
HNT-20CeO_2	10.05 (2.6–17.5)	19.15±0.04	2.55	112
CeO_2	31.0	100.0	–	125

ND* – not determined

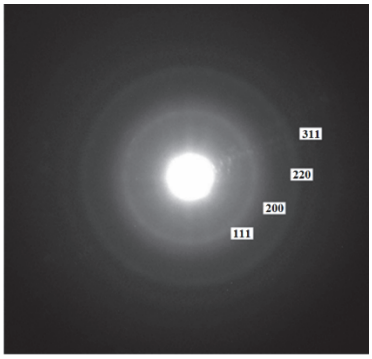

Fig. 3. Electronogram of particles in the nanocomposite is d (hkl) = 3.12 (111), 2.7 (200), 1.89 (220) and 1.64 Å (311)

FTIR spectroscopy is widely used for determining the behavior of the functional groups in halloysite materials. The absorptions bands in the infrared spectrum of halloysite at 3695 and 3622 cm^{-1} are attributed to the stretching vibration of the inner-surface of O–H groups of halloysite. The bands at 3528–3470 cm^{-1} are attributed to the water between the layers. The adsorbed water is indicated by the bending vibration at 1647 cm^{-1}. The stretching mode of Si–O is observed as the peak at 1111 cm^{-1}, while the stretching vibration band of Si–O–Si is observed at 1030 cm^{-1}. The bands between 1000 and 400 cm^{-1} belong to Si–O–Si, Al–O–H, and O–H vibrations (at 796, 754, 689, 539, 469, and 433 cm^{-1}). The typical Si–O-stretching bands of halloysite are at 795 and 754 cm^{-1}. The band observed at 538 cm^{-1} corresponds to the deformation vibration of Al-O-Si. The FTIR spectrum of the halloysite confirms that the band at 912 cm^{-1} belongs to the vibration of the inner surface hydroxyl groups. The peak observed 470 cm^{-1} is due to the deformation vibration of Si-O-Si. The band at 3554 cm^{-1} is assigned to the adsorbed water molecules, while the band at 3603 cm^{-1} is attributed to the isolated water molecules [18–21]. Described structural characteristics are observed in the FTIR spectrum of the studied halloysite. A number of the absorption bands with high reliability of reference to structural fragments are discussed. Fig. 3 shows the FTIR spectra of the studied halloysite. The absorption bands at 3701 and 3631 cm^{-1} in the FTIR spectrum were assigned to the vibration of halloysite Al-OH and Si-OH hydroxyl groups, respectively. Adsorbed water has two signals at 3540 and 3442 cm^{-1} belonging to the stretching vibrations and at 1645 cm^{-1} attributed to bending vibration. The band observed at 2979 cm^{-1} corresponds to the C–H. The region below

1200 cm^{-1} shows bands due to the vibrations of Al-O. The absorptions bands at 1020, 1112, 803, 761, and 712 cm^{-1} attributed to the vibrations of Si-O. The IR spectra of nanocomposites are not significantly different from those of halloysite. No significant differences were found in the spectra of the matrix and modified halloysite nanotubes, and therefore we cannot assert or deny the formation of chemical bonds between Ce oxide and halloysite (Fig. 4).

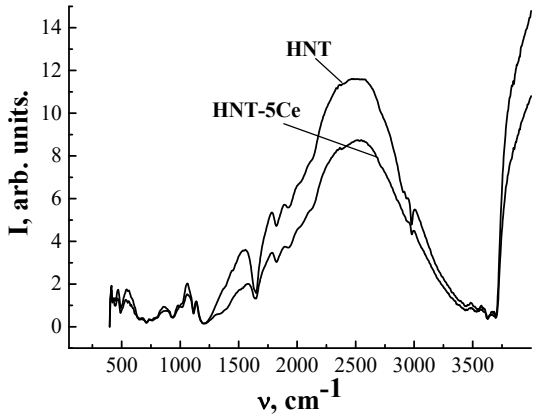

Fig. 4. IR spectra of pristine HNT and nanocomposite HNT-5CeO_2

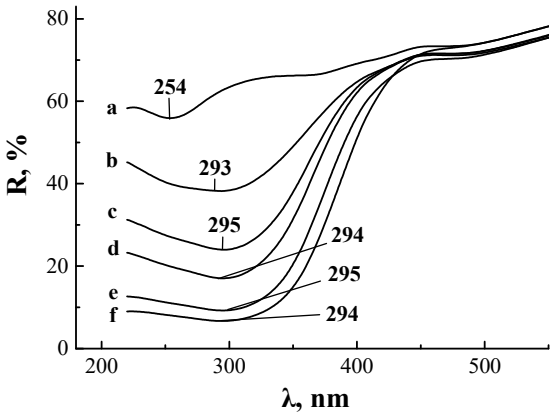

Fig. 5. UV-Vis spectra of pristine HNT (*a*) and nanocomposites HNT-1CeO_2 (*b*), HNT-3CeO_2 (*c*), HNT-5CeO_2 (*d*), HNT-12CeO_2 (*e*), HNT-20CeO_2 (*f*)

Both the size of nanocrystallites and the presence of Ce^{3+} ions on the surface (surface defects) which is characterized by the ratio Ce^{4+}/Ce^{3+} [22] determine the catalytic activity of nanoceria. This was evaluated from the UV spectra of diffuse reflection of HNT and synthesized cerium-containing nanocomposites (Fig. 5). In the spectrum of pristine HNT, a number of maxima (the most intense at 254.2 nm) related to impurities of iron, titanium, and others in aluminosilicate were detected. The content of these ions was determined by energy dispersion analysis. The modification of HNT caused the appearance of a signal from nanoceria in the spectra. Maximum signals at 292.5 nm (HNT-1CeO_2), 294.7 nm (HNT-3CeO_2), 293.7 nm (HNT-5CeO_2), 294.7 nm (HNT-12CeO_2) and 293.7 nm (HNT-20CeO_2) shifted to a long-wavelength region with increasing the content of nanoceria, which confirmed the observations reported elsewhere [23].

The Ce^{4+}/Ce^{3+} ratio was defined as the ratio of the integral signal intensities (Fig. 6 *a*). Mathematical processing of UV-Vis spectra of nanocomposites allowed decomposing the peaks of cerium oxide into two components, corresponding to cerium in different valence states: Ce^{3+} and Ce^{4+} as indicated elsewhere [24–26]. Even though the lower wavelength limit is 220 nm, extrapolating the experimental data to

the unexplored region of the spectrum and its deconvolution into the sum of Gaussian functions, it is possible to distinguish a peak, which we refer to Ce^{4+} [27]. An increase in the content of cerium oxide and, respectively, in nanoparticle diameter results in an increase in the relative content of Ce^{4+} and a decrease in the relative content of Ce^{3+} (Table 2). In the UV-Vis spectrum of cerium nanocomposites, the bands with a maxima located near 207–223 nm are ascribed to Ce^{4+} and the bands with maxima around 310–337 nm to Ce^{3+}. This analysis of UV-Vis spectra is not quantitative; it only allows us to estimate the relative content of the multivalent state of cerium in nanoparticles.

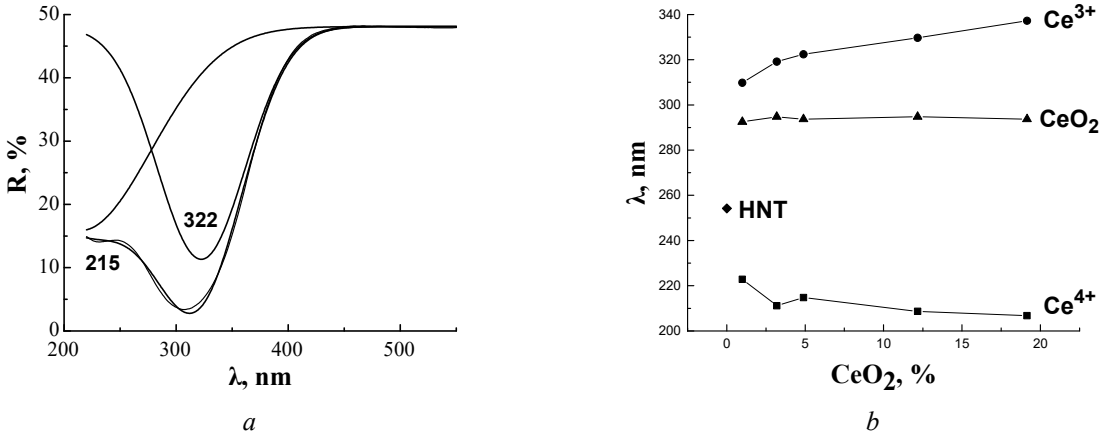

a *b*

Fig. 6. (*a*) – UV-Vis spectrum of cerium(IV) oxide in HNT-5CeO_2 nanocomposites and its decomposition into components, (*b*) – dependence of the peaks maximum position in the UV-Vis spectra of HNT, Ce^{3+}, Ce^{4+}, and CeO_2 on the content of cerium(IV) oxide in nanocomposites

While the position of the band of Ce^{3+} shifts to a longer wavelength (bathochromic shift), the position of the maximum of the band of Ce^{4+} shifts to shorter wavelengths (hypsochromic shift) with increasing the content of CeO_2. The position of the maximum of the total peak, due to the close but differently directed contribution of the Ce^{3+} and Ce^{4+} peaks, does not shift (Fig 6 *b*). At the same time, an increase in the intensity and half-width of the total peak is observed.

As was mentioned before, ceria nanoparticles exhibiting enzyme mimetic activity (catalase and superoxide dismutase). The catalytic activity of pristine HNTs, synthesized nanocomposites with different CeO_2 content (HNT-1CeO_2, HNT-3CeO_2, HNT-5CeO_2, HNT-12CeO_2, and HNT-20CeO_2), a commercial preparation of pure nanoceria and catalase enzyme were determined and compared in a model reaction of hydrogen peroxide decomposition [28] in the pH range of 8.0 to 11.0. The kinetic parameters were calculated based on the Michaelis-Menten equation. Depending on the maximum rate of decomposition of hydrogen peroxide from the catalyst sample in the range of 0.000–0.025 g, a sample from the linear interval with a mass of 0.015 g was selected. The calculated catalytic activity of nanocomposites HNT/CeO_2 was compared with the activity of the enzyme catalase and nanosized cerium oxide calculated by the authors [29, 30].

The activity of the enzyme under these conditions - outside the range of its pH optimum – is low. The catalytic activity of halloysite nanotubes decreasing almost to zero with increasing pH of more than 9. Consequently, the activity of the synthesized nanocomposites in the pH range of 9.5–10.5 is determined by the presence and properties of the decorator – nanosized cerium oxide (Fig. 7). The increase in catalytic activity in the pH range 8.0–10.0 can be associated with an increase in the number of deprotonated ceranol (≡Ce-O^-) groups on the surface of cerium oxide involved in redox reactions of hydrogen peroxide with Ce^{4+} and Ce^{3+} ions. Further increase in the pH leads to a decrease in the catalytic activity of nanomaterials, due to the formation of Ce^{3+} compounds with a low dissociation coefficient on the surface of cerium oxide [31].

It was shown that enzyme catalase demonstrates low catalytic activity in the selected pH range. An extreme dependence of the activity of deposited catalysts on the pH with a maximum at pH range 9.5–10.5 was found (Fig. 6). The catalytic activity of HNT (a carrier of the decorator in the synthesized nanocomposites) decreased with increasing pH. We can assume that the activity of the synthesized nanocomposites at pH range 9.0–11.0 is determined by the presence and properties of a decorator – nanoceria.

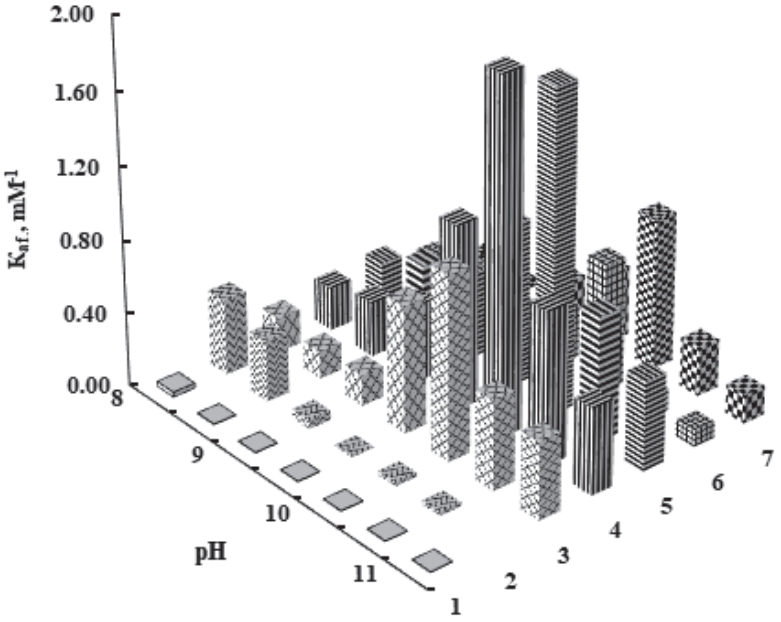

Fig. 7. Dependence of the catalytic activity of materials (K_{af}) on the pH in the reaction of hydrogen peroxide decomposition: *1* – Catalase, *2* – HNT, *3* – HNT-1Ce, *4* – HNT-3Ce, *5* – HNT-5Ce, *6* – HNT-12Ce, *7* – HNT-20Ce

An extreme dependence of the activity on the content of the decorator with a maximum for the sample of 3.19 % CeO_2 was found (Fig. 8). We assume that this nanocomposite has both a small particle size and, consequently, a high surface area, as well as a small ratio of Ce^{4+} to Ce^{3+} (1.17), which leads to an increase in the catalytic activity of the sample.

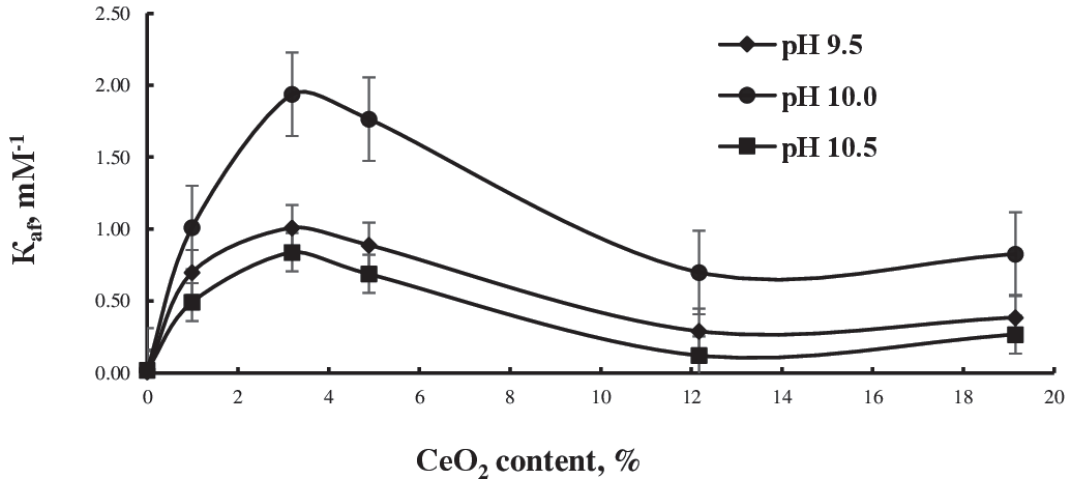

Fig. 8. Dependence of nanomaterials activity on the CeO_2 content

In the CeO_2 content range from 0 to 3.19 %, the catalytic activity of nanocomposites is almost directly proportional to the content of the decorator. An increase in the content of CeO_2 leads to the aggregation of particles, a decrease in their specific surface area, which leads to a decrease in the number of surface defects (the measure of which is the ratio (Ce^{4+}/Ce^{3+}) (Fig. 9).

Recalculation of the catalytic capability of nanocomposites to 100 % of the content of the decorator in them (Fig. 10) makes it possible to analyze the factors that determine the activity of nanoceria. In terms of 100 % cerium oxide content, the best catalytic activity is shown by the sample HNT-1CeO_2, which contains 0.99 % of the modifier and has a ratio of Ce^{4+}/Ce^{3+} 0.25 (Table 2).

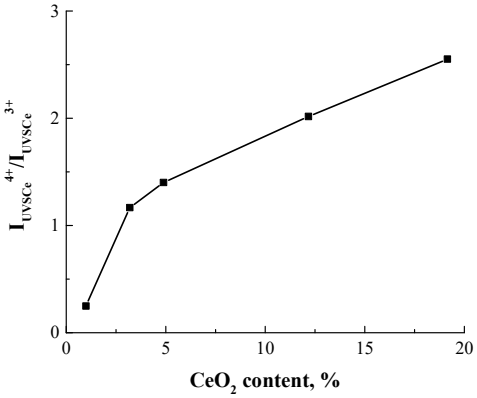

Fig. 9. Dependence of the ratio of the ratio of $I_{UVSCe}{}^{4+}/I_{UVSCe}{}^{3+}$ on the content of CeO_2

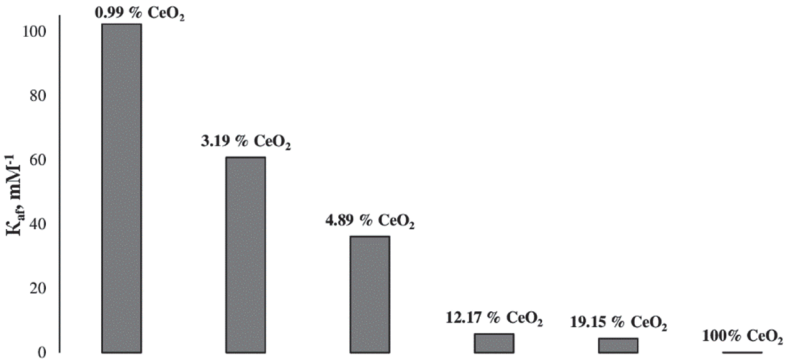

Fig. 10. The activity of nanocomposites at pH 10.0 in terms of 100 % content of cerium oxide

The activity of nanoceria in nanocomposites decreases with increasing Ce^{4+}/Ce^{3+} ratio (Fig. 11), i.e. with decreasing the number of oxygen vacancies; activity decreases with increasing cerium oxide content due to aggregation of nanocrystallites; the activity decreases with increasing particle diameter due to the reduction of the surface.

The activation energies (E_a) of the reaction of hydrogen peroxide decomposition by the nanocomposites and pristine HNT in the temperature range of 20–40 °C at pH 10 were obtained by plotting the logarithm of the rate constant (k), versus the inverse temperature ($1/T$).

The dependence of the activation energy of the decomposition reaction of hydrogen peroxide by nanocomposites HNT-cerium oxide on the content of CeO_2 and the ratio of $I_{UVSCe}{}^{4+}/I_{UVSCe}{}^{3+}$ has shown that the effective activation energy for pristine HNT is 170 kJ/mol (Fig. 12). The activation energy decreased from 154 kJ/mol for the material with the lowest modifier content to 112 kJ/mol for the nanocomposite with the highest amount of a modifier (Table 2). Despite expectations, the effective activation energy of the decomposition reaction of hydrogen peroxide does not decrease with increasing defect of ceria nanocrystallites in nanocomposites but decreases with increasing the content of nanoceria (%) in nanocomposites (Fig. 1).

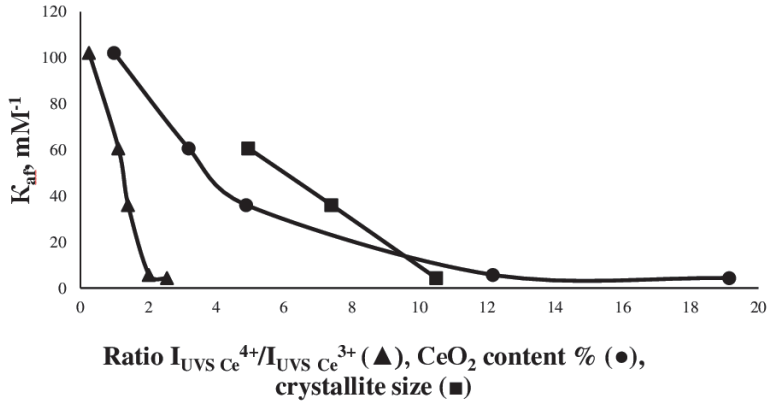

Fig. 11. The activity of nanocomposites at pH 10.0 as dependent on the ratio of Ce^{4+}/Ce^{3+} (▲), CeO_2 content, %(●), and CeO_2 nanocrystallites size, nm (■)

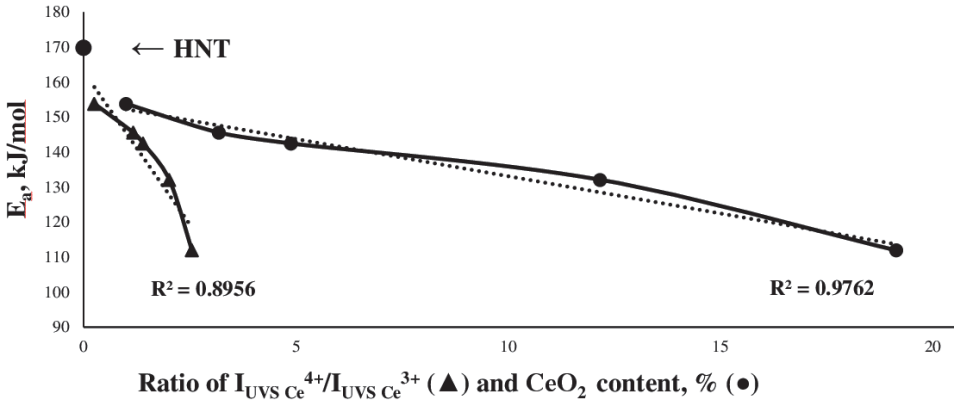

Fig. 12. Dependence of the activation energy of the decomposition reaction of hydrogen peroxide by nanocomposites of HNT-cerium oxide on the content of CeO_2 (●) and the ratio of $I_{UVSCe}^{4+}/I_{UVSCe}^{3+}$ (▲)

CONCLUSION

A number of composite HNT-Cerium oxide-based materials were synthesized via deposition reaction using aqueous cerium nitrate solutions without any stabilizers at room temperature. The characteristics of the studied materials are determined by physical and chemical analysis methods. The content of cerium oxide in the synthesized samples was 0.99, 3.19, 4.89, 12.17 and 19.15 wt. %. Electron microscopy showed that the size of CeO_2 particles varied in the range of 2.6–17.5 nm. According to the results of the X-ray phase analysis, cerium dioxide has a cubic structure. The characteristics of the porous structure were determined based on low-temperature nitrogen adsorption/desorption isotherms. The specific surface area ranged from 31 to 54 m^2/g. IR spectroscopy determined the type of interaction between the modifier and the matrix. The $I_{UVS\ Ce}^{4+}/I_{UVS\ Ce}^{3+}$ ratio in nanocomposites was estimated from UV-spectra of diffuse reflectance; it varied in the range of 0.25 to 2.55. The catalytic activity of the synthesized materials and halloysite nanotubes was determined by calculating the affinity constant from kinetic data of the model reaction of hydrogen peroxide decomposition in the pH range of 8.0 to 11.0 and compared to the catalase enzyme and commercial nanosized CeO_2. The catalytic activity of pristine HNT decreased with increasing pH. We can assume that the activity of the synthesized nanocomposites at pH range 9.0–11.0 is determined by the presence and properties of a decorator – nanoceria. The pH dependence of the activity of the nanocomposites was shown to be extreme with the maximum in the pH range of 9.5–10.5. An extreme dependence of the activity on the content of the decorator with a maximum for the sample of 3.19 % wt. CeO_2 was found.

Recalculation of the catalytic capability of nanocomposites to 100 % of the content of the decorator in them makes it possible to analyze the factors that determine the activity of nanoceria. Under these conditions, the best catalytic activity demonstrates by the sample HNT-1CeO_2, which contains 0.99 % wt. of the modifier and has a ratio of Ce^{4+}/Ce^{3+} 0.25. It has been found that the activity of nanoceria in nanocomposites decreases with: increasing Ce^{4+}/Ce^{3+} ratio, i.e. with decreasing the number of oxygen vacancies; with increasing cerium oxide content - due to aggregation of nanocrystallites; and with increasing particle diameter due to the reduction of the surface. The activation energy (E_a) of the reaction of hydrogen peroxide decomposition by the nanocomposites and pristine HNT in the temperature range of 20–40 °C at pH 10 was determined by kinetic data. The E_a for pristine HNT is 170 kJ/mol. It has been shown that the increasing content of nanoceria in nanocomposites leads to a decrease in the activation energy of the reaction of hydrogen peroxide decomposition from 154 kJ/mol for the material with the lowest modifier content to 112 kJ/mol for the nanocomposite with the highest amount of a modifier.

Розкладання пероксиду водню нанокомпозитами галоїзитні нанотрубки/оксид церію

А.М. Гринько, А.В. Бричка, О.М. Бакалінська, Г.О. Каленюк, М.Т. Картель

Національний університет «Києво-Могилянська академія»
вул. Сковороди, 2, Київ, 04070, Україна, alinagrinko2@gmail.com
Інститут хімії поверхні ім. О.О. Чуйка Національної академії наук України
вул. Олега Мудрака, 17, Київ, 03164, Україна, bakalin2008@ukr.net

Методом осадження водного розчину нітрату церію за кімнатної температури без стабілізаторів, за присутності носія було синтезовано ряд наноматеріалів на основі галоїзитних нанотрубок (ГНТ), декорованих CeO_2. Кількість нанесеного нанооксиду церію варіюється від 0.99 до 19.15 мас. %. За даними електронної мікроскопії, розмір частинок CeO_2 варіюється в межах 2.6–17.5 нм. Рентгеноструктурний аналіз зразків показав кубічну структуру діоксиду церію. Характеристики пористої структури визначали за низькотемпературними ізотермами адсорбції/десорбції азоту. Питома поверхня змінюється у межах від 31 до 54 м^2/г. ІЧ-спектроскопією визначено тип взаємодії модифікатора з матрицею. Співвідношення $I_{UVS\,Ce^{4+}}/I_{UVS\,Ce^{3+}}$ в нанокомпозитах, визначене за УФ-спектрами дифузного відбиття, варіюється в діапазоні від 0.25 до 2.55. Каталітичну активність синтезованих матеріалів і вихідних галоїзитних нанотрубок визначали розрахунком констант аффінності з кінетичних даних модельної реакції розкладання пероксиду водню в діапазоні pH від 8.0 до 11.0 і порівнювали з ферментом каталазою та комерційним нанорозмірним CeO_2. Каталітична активність вихідних ГНТ знижувалася зі збільшенням pH, що дозволяє припустити, що активність синтезованих нанокомпозитів в діапазоні pH 9.0–11.0 визначається наявністю та властивостями декоратора – наноцерію. Показано, що pH-залежність активності нанокомпозитів є екстремальною з максимумом в діапазоні pH 9.5–10.5. Встановлено також екстремальну залежність активності від вмісту декоратора з максимумом для зразка що містить 3.19 мас. % CeO_2. Перерахунок каталітичної здатності нанокомпозитів на 100 % вміст декоратора дає змогу проаналізувати фактори, що визначають активність наноцерію. За цих умов найкращу каталітичну активність демонструє зразок ГНТ-1CeO_2, який містить 0.99 мас. % модифікатора та має співвідношення Ce^{4+}/Ce^{3+} 0.25. Встановлено, що активність наноцерію в нанокомпозитах зменшується: зі збільшенням співвідношення Ce^{4+}/Ce^{3+}, тобто зі зменшенням кількості вакансій кисню; зі збільшеням вмісту оксиду церію – за рахунок агрегації нанокристалітів; зі збільшенням діаметра частинок через зменшення поверхні. За кінетичними даними визначено енергію активації (E_a) реакції розкладання пероксиду водню нанокомпозитами та вихідними ГНТ в інтервалі температур 20–40 °C при pH 10. E_a для вихідних ГНТ становить 170 кДж/моль. Показано, що збільшення вмісту наноцерію в нанокомпозитах приводить до зменшення енергії активації реакції розкладання пероксиду водню від 154 кДж/моль для матеріалу з найменшим вмістом декоратора до 112 кДж/моль для нанокомпозиту з найбільшою кількістю декораатора.

***Ключові слова**: наночастинки оксиду церію, галоїзитні нанотрубки, нанокомпозити, каталітична активність, розкладання пероксиду водню, енергія активації*

REFERENCES

1. Cheng C., Song W., Zhao Q., Zhang H. Halloysite nanotubes in polymer science: purification, characterization, modification and applications. *Nanotechnol. Rev.* 2020. **9**(1): 323.
2. Satish S., Tharmavaram M., Rawtani D. Halloysite nanotubes as a nature's boon for biomedical applications. *Nanobiomedicine (Rij).* 2019. **6**: 1849543519863625.
3. Yuan P., Tan D., Annabi-Bergaya F. Properties and applications of halloysite nanotubes: recent research advances and future prospects. *Appl. Clay Sci.* 2015. **112–113**: 75.
4. Prishchenko D., Zenkov E., Mazurenko V., Fakhrullin R., Lvov Y., Mazurenko V. Molecular dynamics of the halloysite nanotubes. *Phys. Chem. Chem. Phys.* 2018. **20**: 5841.
5. Mahajan A., Gupta P. Halloysite nanotubes based heterogeneous solid acid catalysts. *New J. Chem*. 2020. **44**(30): 12897.
6. Danyliuk N., Tomaszewska J., Tatarchuk T. Halloysite nanotubes and halloysite-based composites for environmental and biomedical applications. *J. Mol. Liq.* 2020. **309**: 113077.
7. Massaro M., Colletti C.G., Lazzara G., Milioto S., Noto R., Riela S. Halloysite nanotubes as support for metal-based catalysts. *J. Mater. Chem. A.* 2017. **5**(26): 13276.
8. Lvov Y., Panchal A., Fu Y., Fakhrullin R., Kryuchkova M., Batasheva S., Stavitskaya A., Glotov A., Vinokurov V. Interfacial self-assembly in halloysite nanotube composites. *Langmuir.* 2019. **35**(26): 8646.
9. Tang J.L.Y., Moonshi S.S., Ta H.T. Nanoceria: an innovative strategy for cancer treatment. *Cell. Mol. Life Sci.* 2023. **80**(2): 46.
10. Brandão Da Silva Assis M., De Moraes G.N., De Souza K.R. Cerium oxide nanoparticles: Chemical properties, biological effects and potential therapeutic opportunities (Review). *Biomed. Rep.* 2024. **20**(3): 48.
11. Othman A., Gowda A., Andreescu D., Hassan M.H., Babu S.V., Seo J., Andreescu S. Two decades of ceria nanoparticle research: structure, properties and emerging applications. *Mater Horiz*. 2024. **11**(14): 3213.
12. Feng Y., Luo X., Li Z., Fan X., Wang Y., He R.R., Liu M. A ferroptosis-targeting ceria anchored halloysite as orally drug delivery system for radiation colitis therapy. *Nat. Commun.* 2023. **14**(1): 5083.
13. Almofty S., Ravinayagam V., Alghamdi N., Alghamdi W., Albazroun Z., Almulla L., Akhtar S., Almofleh A.A., Tanimu G., Dafalla H., Jermy B.R. Effect of CeO_2/spherical silica and halloysite nanotubes engineered for targeted drug delivery system to treat breast cancer cells. *OpenNano*. 2023. **13**: 100169.
14. Chen L., Wang Q., Wang X., Cong Q., Ma H., Guo T., Li S., Li W. High-performance CeO_2/halloysite hierarchical catalysts with promotional redox property and acidity for the selective catalytic reduction of NO with NH_3. *Chem. Eng. J.* 2020. **390**: 124251.
15. Qureshi A., Habib S., Nawaz M., Shakoor R., Kahraman R., Ahmed E. Modified halloysite nanotubes decorated with Ceria for synergistic corrosion inhibition of Polyolefin based smart composite coatings. *Appl. Clay Sci.* 2023. **233**: 106827.
16. Chakraborty T., Yadav D., Bedar A., Pandey M., Saxena S., Shukla S. PVDF-Halloysite-Ceria Multifunctional Membrane for One-step Treatment to Industrial Effluent. *J. Environ. Chem. Eng.* 2024. **12**(3): 112936.
17. Brychka S., Hedin N., Brychka A. Halloysite Nanotubes Modified with Nanoparticles of Cerium Oxide for Ultraviolite Protection. Available at SSRN: https://ssrn.com/abstract=4446720 or http://dx.doi.org/10.2139/ssrn.4446720
18. Bordeepong S., Bhongsuwan D., Pungrassami T., Bhongsuwan T. Characterization of halloysite from Thung Yai District, Nakhon Si Thammarat Province, in Southern Thailand. *Songklanakarin J. Sci. Technol.* 2011. **33**(5): 599.
19. Aytekin M.T., Hoşgün H.L. Characterization studies of heat-treated halloysite nanotubes. *Chem. Pap.* 2020. **74**: 4547.
20. Gaaz T.S., Sulong A.B., Kadhum A.A.H., Al-Amiery A.A., Nassir M.H., Jaaz A.H. The Impact of Halloysite on the Thermo-Mechanical Properties of Polymer Composites. *Molecules*. 2017. **22**(5): 838.
21. Khunova V., Kristof J., Kelnar I., Dybal J. The effect of halloysite modification combined with in situ matrix modifications on the structure and properties of polypropylene/halloysite nanocomposites. *eXPRESS Polym. Lett.* 2013. **7**(5): 471.
22. Vinothkumar G., Arunkumar P., Mahesh A., Dhayalan A., Suresh Babu K. Size- and defect-controlled anti-oxidant enzyme mimetic and radical scavenging properties of cerium oxide nanoparticles. *New J. Chem.* 2018. **42**(23): 18810.
23. Lin K.S., Chowdhury S. Synthesis, characterization, and application of 1-D cerium oxide nanomaterials: a review. *Int. J. Mol. Sci.* 2010. **11**(9): 3226.
24. Rosero-Navarro N.C., Figiel P., Jedrzejewski R., Biedunkiewicz A., Castro Y., Aparicio M., Pellice S.A., Duran A. Influence of cerium concentration on the structure and properties of silica-methacrylate sol–gel coatings. *J. Sol-Gel Sci. Technol.* 2010. **54**(3): 301.

25. Calvache-Muñoz J., Prado F.A., Rodríguez-Páez J.E. Cerium oxide nanoparticles: synthesis, characterization and tentative mechanism of particle formation. *Colloids Surf., A*. 2017. **529**: 146.
26. Elkhoshkhany N., Khatab M.A., Kabary M.A. Thermal, FTIR and UV spectral studies on tellurite glasses doped with cerium oxide. *Ceram. Int.* 2018. **44**(3): 2789.
27. Brandily-Anne M.-L., Lumeau J., Glebova L., Glebov L.B. Specific absorption spectra of cerium in multicomponent silicate glasses. *J. Non-Cryst. Solids*. 2010. **356**(44–49): 2337.
28. Grinko A.M., Brichka A.V., Bakalinska O.M., Oranska O.I., Kartel M.T. Kaolin/cerium oxide nanocomposites: properties and activity in hydrogen peroxide decomposition reaction. *Voprosy khimii i khimicheskoi tekhnologii*. 2020. **3**: 59.
29. Glevatska K.V., Bakalinska O.M., Tarasenko Yu.O., Kartel M.T. Catalytic (enzyme-like) properties of multilayer carbon nanotubes. *Kharkov University Bulletin.* 2010. **18**(41): 248. [in Ukrainian].
30. Dmytrenko T.Yu., Kulyk K.S., Voitko K.V., Bakalinska O.N., Borysenko N.V., Kartel M.T. Catalytic activity of cerium-containing materials in reaction of hydrogen peroxide decomposition. *Him. Fiz. Tehnol. Poverhni.* 2014. **5**(3): 317. [in Ukrainian].
31. Vlasova N.N., Golovkova L.P., Stukalina N.G. Adsorption of organic acids on a cerium dioxide surface. *Colloid J.* 2015. **77**: 418.

Received 14.04.2025, accepted 04.09.2025